Investigation of Orientation and Relaxation in a Segmented Zwitterionomer by Fourier Transform Infrared Spectroscopy

Yanxiang Wang, C. Geraldine Bazuin,* and Michel Pézolet*

Centre de Recherche en Sciences et Ingénierie des Macromolécules, Département de chimie, Université Laval, Cité universitaire, Québec, Canada G1K 7P4

Received April 26, 2001

ABSTRACT: The orientation behavior of a segmented poly(tetramethylene oxide) (PTMO) zwitterionomer, with a narrow polydispersity PTMO segmental molecular weight of 5.2×10^3, a melting point of 17 °C, and elastomeric characteristics, was studied using infrared linear dichroism. The results obtained show that when the amorphous zwitterionomer is stretched at ambient temperature, the PTMO chains orient in the stretch direction. At a draw ratio of approximately 3, strain-induced crystallization occurs and increases with strain amplitude. The chain axis of the crystallized PTMO segments are almost perfectly oriented in the stretch direction, whereas the orientation of the amorphous segments is low and undergoes no further changes during crystallization. The degree of crystallization was also determined from the spectra (22% for a draw ratio of 5.6). The crystallization kinetics were shown to follow the Avrami equation, indicating one-dimensional growth ($n = 0.8$). Orientation relaxation following deformation was also studied as a function of temperature at draw ratios and temperatures where strain-induced crystallization is avoided. Little orientation was detected in the ionic regions of the polymer during stretching. The orientation function for the PTMO soft blocks decreases, and the relaxation rate increases with increasing temperature. Time−temperature superposition of the relaxation curves is discussed in relation to the hard (or cluster) phase transition.

Introduction

Ionomers are a well-known class of thermoplastic polymers containing a relatively small percentage of ionic functional groups in a matrix of low dielectric constant.[1−3] They may be based on a wide variety of polymers or copolymers, including rubbery ones such as polybutadiene, glassy ones such as polystyrene (PS) and poly(methyl methacrylate) (PMMA), and partially crystalline ones such as polyethylene (PE) and polypropylene (PP). The morphology and properties of the bulk ionomers have been studied extensively using techniques such as small-angle X-ray and neutron scattering (SAXS and SANS), dynamic mechanical analysis (DMA), differential scanning calorimetry (DSC), and transmission electron microscopy (TEM). The results obtained indicate that the ionic units associate due to electrostatic forces, producing nanometer-size ionic aggregates termed "multiplets", which are dispersed in the weakly polar polymer matrix; these give rise to regions of reduced mobility that form the basis of the so-called "cluster phase" (hard phase) having a higher glass transition (T_g) than the matrix phase (soft phase).[1,3,4]

Zwitterionomers are electrically neutral ionomers that carry an equal number of positively and negatively charged sites linked through covalent bonds.[1,5] A series of homologous *segmented* zwitterionomers of the type shown in Scheme 1 were synthesized by Grassl and Galin[6] and their bulk properties and structure analyzed.[7−9] Their chain topology is characterized by the regular alternation of strongly polar zwitterionic short junctions and weakly polar poly(tetramethylene oxide) (PTMO) segments of well-controlled molecular weight and low polydispersity. The zwitterionomers with longer PTMO segments ($M_n > 3 \times 10^3$) are semicrystalline, with melting points ranging from about 10 to 25 °C.[7]

Scheme 1

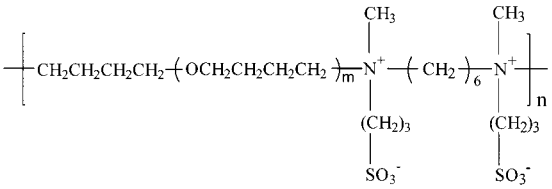

The amorphous zwitterionomers display the typical biphasic behavior of ionomers, with two (DSC-detectable) T_g's and reduced mobility regions around the zwitterionic multiplets (detected by solid-state NMR).[7] The phase segregation is strong (sharp interfaces), resulting in a pure PTMO soft phase ($T_g = -75$ °C) and a hard phase ($T_g = -5$ to 40 °C) containing about 10−30% of the PTMO (involving 2−3 neighboring TMO units per zwitterion).[7,8] The semicrystalline zwitterionomers above their melting points are phase-separated like the amorphous ones, but with concomitantly smaller rigid fractions.[7] The relative stability of the zwitterionic multiplets to high temperatures well beyond the cluster transition confers substantial elastic character to these materials, in particular those with the longer PTMO segments, which show an entropic increase in modulus with temperature.[9] Finally, the multipeak SAXS diagrams of the PTMO zwitterionomers indicate the existence of long-range order in these materials, which generally display lamellar or hexagonal morphologies.[8]

The well-defined character and the properties of these materials make them interesting candidates for orientation and relaxation behavior studies. Moreover, because of the presence of a melting point near ambient temperature, strain-induced crystallization can be expected and thus easily investigated. Strain-induced crystallization is well-known to occur in stretched elastomers due to the conformational entropy decrease of the

* To whom correspondence should be addressed.

10.1021/ma0107197 CCC: $20.00
Published on Web 07/27/2001

elongated chains.[10,11] Studies of this phenomenon and of orientation and relaxation behavior in general are important for both industrial applications and a fundamental understanding of the often complex processes involved. Such investigations have been made using approaches that provide information at the macroscopic level (e.g., mechanical properties and birefringence behavior)[12−19] as well as using various spectroscopic techniques such as fluorescence polarization,[20,21] nuclear magnetic resonance,[22] and infrared spectroscopy[10,16,23−37] that probe the *submolecular* level response of polymeric networks and melts to deformation.

For the present study, we have chosen the semicrystalline PTMO zwitterionomer shown in Scheme 1; it is characterized by a melting point that is a few degrees below ambient temperature,[7] and it is elastomeric to well above its melting point (see Experimental Section for details). Its orientation and relaxation behavior, including strain-induced crystallization, is investigated using infrared linear dichroism (IRLD). With this single technique, various aspects of the strain-induced crystallization behavior in this polymer are studied, including the orientation of the crystalline domains, the degree of crystallinity, and the crystallization kinetics. Furthermore, the orientation in the amorphous domains before and during crystallization is followed. The orientation relaxation behavior in a temperature and strain range where no crystallization occurs is also investigated.

Experimental Section

Sample Characteristics and Preparation. The zwitterionomer used (Scheme 1) was synthesized in the laboratory of Dr. J.-C. Galin (Institut Charles Sadron, Strasbourg, France) and characterized by NMR spectroscopy, size exclusion chromatography, thermogravimetric analysis, etc.[6] The PTMO blocks have a number-average molecular weight (M_n) of 5.19 $\times$ 10^3 (M_w/M_n < 1.15). The zwitterionomer has a weight-average chain extension degree of 54 and a polydispersity index of 2. It contains about 0.074 (weight fraction) of highly polar zwitterionic units. DSC measurements indicate a soft-phase glass transition of −75 °C and a melting point of 17 °C; a hard-phase (cluster) T_g is detected at 44 °C (with a width of 33 °C) when crystallization is avoided.[7] According to DMA (1 Hz), the zwitterionomer is elastomeric (increasing rubbery modulus; log $E' \sim 6.7$ Pa) up to about 100 °C.[9] SAXS data indicate a hexagonal morphology.[8,38]

Thin films were prepared by solution casting from a 5% binary mixture of chloroform and trifluoroethanol (9:1 by volume) onto a Teflon film. They were dried at 45 °C under vacuum for about 3 weeks to remove residual solvent. It was verified in the infrared spectra that no solvent peaks were present. The sample/Teflon film was cut into strips with a new razor blade, and then the zwitterionomer films were peeled off the substrate with great care to avoid induced orientation. Both ends of the films were wrapped in strips of pyrotape (Aremco Products No. 546) to prevent sample slippage in the jaws of the stretcher during stretching. Before stretching, the position of the jaws of the stretcher was manually adjusted so that the film was fully extended. The sample sizes before stretching were 1 cm in length, 0.8 cm in width, and about 30 μm in thickness. To ensure comparable results for the various experimental conditions, all strips measured were taken from the same sample/Teflon film.

Poly(tetramethylene oxide) of molecular weight 2900 (commercial name is Terathane 2900) was purchased from Sigma-Aldrich Canada. The FTIR spectrum of amorphous PTMO was obtained after melting the sample on the surface of a KBr disk. The FTIR spectrum of crystallized PTMO was taken after about 1 day of isothermal crystallization of the PTMO melt at ambient temperature.

Infrared Spectroscopy. The FTIR spectra were recorded using a Nicolet Magna 560 spectrometer equipped with a narrow band MCT detector. The spectral resolution was 4 cm^{-1}, and each spectrum was obtained by coadding four interferograms with a total measurement time of about 2 s for each spectrum. The treatment of the infrared spectra was done using Grams 5.1 (Galactic Industries). The absorbance was determined by measuring the area under the band after drawing a linear baseline between the appropriate minima.[39] For curve fitting, a linear baseline was also used, and the line shape of the resolved peaks was found to remain constant regardless of the draw ratio.

For the study of the orientation and strain-induced crystallization behavior at ambient temperature, the zwitterionomer film was stretched step-by-step in equal time intervals up to a maximum draw ratio of 5.6. In each step, the film was fast stretched (99 mm/min) to a constant length, and the polarized infrared spectra were measured after about 2 min of the onset of stretch. It should be noted that it is necessary to maintain an equal time interval in each step between the onset of stretch and the start of the measurements because orientation and strain-induced crystallization are not thermodynamic equilibrium processes, which means that the orientation and strain-induced crystallization change as a function of time after the onset of strain. After the maximum strain, the film was released to the original length in the same manner. The elongation−retraction cycle was repeated three times on the same sample.

For the orientation relaxation measurements, a mechanical stretcher head fitted with ZnSe windows was installed inside the sample compartment, and the inner temperature was controlled by an Omega temperature controller (CN7600) and heating cartridges. For all measurements, the stretching rate was adjusted to 99 mm/min. After the film was stretched to the desired length L (giving the draw ratio, $\lambda = L/L_0$, where L_0 is the unstretched length), the polarized infrared spectra were recorded in situ. The spectrum with polarized radiation parallel to the stretch direction was first measured, then the ZnSe wire-grid polarizer (Specac) was automatically rotated by 90°, and the perpendicularly polarized spectrum was collected. The time interval between the recording of the two polarized spectra was about 12 s.

Infrared Linear Dichroism (IRLD). IRLD is based on the measurement of either the dichroic ratio $R(\bar{\nu}) = A_{\parallel}(\bar{\nu})/A_{\perp}(\bar{\nu})$ or the dichroic difference $\Delta A(\bar{\nu}) = A_{\parallel}(\bar{\nu}) - A_{\perp}(\bar{\nu})$, where $A_{\parallel}(\bar{\nu})$ and $A_{\perp}(\bar{\nu})$ are the absorbances of the band centered at wavenumbers $\bar{\nu}$, measured with the polarized infrared radiation parallel and perpendicular to the stretch direction, respectively.[40] In the case of a cylindrically symmetric distribution of the functional groups, the orientation of the transition moment vector of a normal vibration with respect to the stretch direction may be expressed in terms of the second Legendre polynomial $\langle P_2(\cos\gamma)\rangle$, which is related to the dichroic ratio R, the dichroic difference ΔA, and the isotropic absorbance A_0 by the following equation:

$$\langle P_2(\cos\gamma)\rangle = \frac{3\langle\cos^2\gamma\rangle - 1}{2} = \frac{R-1}{R+2} = \frac{\Delta A}{3A_0} \qquad (1)$$

In this study, the orientation function $\langle P_2(\cos\gamma)\rangle$ was calculated from the dichroic ratio since this parameter is independent of the thickness of the sample. For an isotropic sample, $\langle P_2(\cos\gamma)\rangle = 0$. For an oriented sample, $\langle P_2(\cos\gamma)\rangle = 1$ if all transition moments are perfectly oriented in the reference direction (stretch direction), while $\langle P_2(\cos\gamma)\rangle = 0$ and −0.5 for a perfect orientation at $\gamma = 54.7°$ and 90°, respectively.

Results and Discussion

The ambient-temperature infrared spectra of the unoriented PTMO zwitterionomer and a pure PTMO melt are shown in Figure 1. The difference between the two spectra is also shown in this figure in order to determine the absorptions from the ionic short blocks.

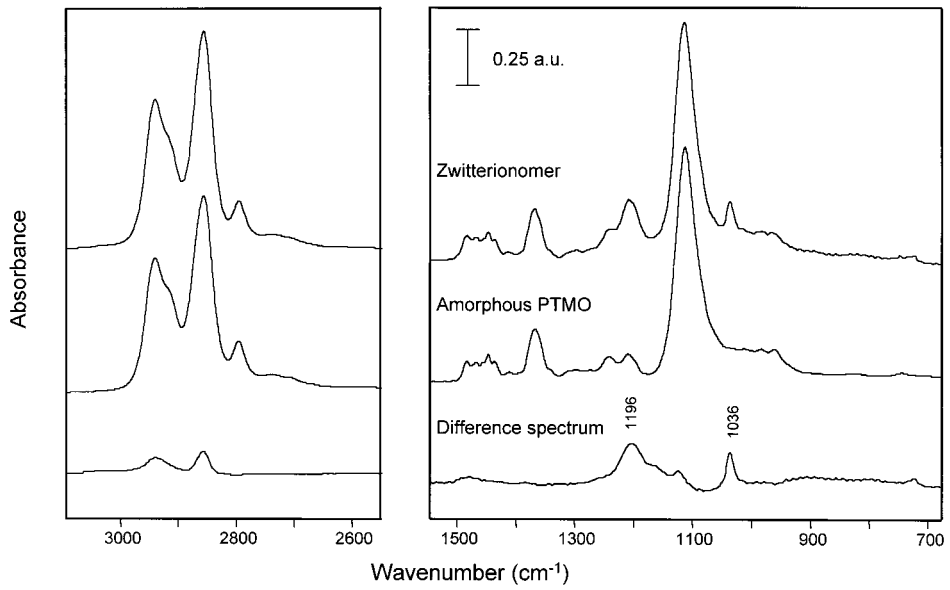

Figure 1. FTIR spectra of the isotropic PTMO zwitterionomer, a pure PTMO melt, and the difference between the two spectra.

Table 1. Assignments of the Infrared Bands of the PTMO Zwitterionomer[a]

wavenumber (cm^{-1})			
amorphous zwitterionomer	semicrystalline zwitterionomer[b]	semicrystalline PTMO	assignts[d]
2940 (⊥)	2941 (⊥)	2941	$\nu_a(CH_2)$
2916 (⊥)	2916 (⊥)	2916	$\nu_a(CH_2)$
2855 (⊥)	2863 (⊥)	2863	$\nu_s(CH_2)_2$
2796 (⊥)	2804 (⊥)	2804	$\nu_s(CH_2)_1$
1483 (⊥)	1491 (⊥)	1491	$\delta(CH_2)_1$
1467 (∥)	1475 (∥)	1475	$\delta(CH_2)_1$
1455 (∥)	1460 (∥)	1460	$\delta(CH_2)_2$
1447 (∥)	1447 (∥)	1447	$\delta(CH_2)_2$
1368 (∥)	1371 (∥)	1372	$\omega(CH_2)_1$
1242 (∥)	1251 (∥)	1251	$\omega(CH_2)_2$
	1234 (∥)	1234	$\omega(CH_2)_2$
1208 (⊥)	1210 (⊥)	1209	$t(CH_2)$
1197 (?)[c]	1196 (?)[c]		$\nu_a(SO_3^-)$
1112 (∥)	1112 (∥)	1112	$\nu_a(COC)$
1036 (?)[c]	1036 (?)[c]		$\nu_s(SO_3^-)$
	1011 (∥)	1010	skeletal stretching
	997 (∥)	996	$\nu_s(COC)$
	746 (∥)	746	$r(CH_2)$

[a] The $(CH_2)_1$ and $(CH_2)_2$ represent the α and β methylenes in PTMO ($O-C^{\alpha}H_2-C^{\beta}H_2$), respectively. [b] Stretched to a draw ratio of 5.6 at ambient temperature. [c] Bands associated with the ionic aggregates. [d] ν = stretching, ν_a = antisymmetric stretching, ν_s = symmetric stretching, δ = bending, ω = wagging, t = twisting, r = rocking, τ = torsion, ⊥ = stronger in perpendicular polarization, ∥ = stronger in parallel polarization.

To obtain the difference spectrum, a subtraction factor determined by trial-and-error was used to eliminate the bands due to the PTMO segments. The assignment of the observed bands, based on the best evidence available at the present time,[41,42] is given in Table 1, along with those for unoriented semicrystalline PTMO and a stretched partly crystallized zwitterionomer. Clearly, bands assigned to different segments and phases of the polymers are distinguished and can thus be used to study the segmental response to macroscopic deformation. Among the infrared absorption bands of the ionic short blocks, only two strong absorptions at about 1036 and 1196 cm^{-1} are isolated from those of PTMO; they are assigned to the SO_3^- symmetric and antisymmetric stretching vibrational modes, respectively.

Orientation and Strain-Induced Crystallization. Figure 2 shows the polarized infrared spectra of the PTMO zwitterionomer at maximum elongation (draw ratio of 5.6) in the first elongation−retraction cycle. For comparison, the infrared spectrum of the semicrystalline PTMO sample is included. The dichroic difference spectra ($\Delta A = A_{\parallel} - A_{\perp}$) at each stretching step in the first cycle are plotted on the same scale in Figure 3. The appearance and growth of the crystalline bands, which are much narrower and display a much higher dichroism than the amorphous PTMO bands, clearly indicate that stretching the zwitterionomer at ambient temperature induces crystallization of the PTMO moiety of the polymer. Judging from the appearance of the purely crystalline bands at 997 and 1011 cm^{-1}, which are not affected by other bands, the sample begins to crystallize at a draw ratio of about 3 in the experimental conditions used. It is noted that the PTMO band positions in the crystallized zwitterionomer are essentially identical to those of the semicrystalline PTMO homopolymer.

The bands related to the CH_2 stretching modes in the 3000−2750 cm^{-1} region (Figure 3) show highly negative dichroism at high draw ratios and give band shapes similar to that of crystallized PTMO, indicative of crystalline segments in fully trans conformation. This indicates that the crystallized PTMO segments in the zwitterionomer are extended in trans conformation, with the chain axis oriented in the stretch direction. The high dichroism of the purely crystalline bands at 1011 cm^{-1}, which is present only in the parallel polarized spectrum, and at 997 cm^{-1}, which is present only in the perpendicularly polarized spectrum, indicates that the orientation of the crystalline segments in the stretch direction is almost perfect.

Compared with the PTMO bands, those due to the ionic blocks at about 1196 and 1036 cm^{-1} display a considerably smaller dichroism even at high deformation. [The small bipolar band character of the 1036 cm^{-1} band at low draw ratio (Figure 3) is caused by a small wavenumber shift of this band after stretch.] Although some order may exist in the ionic aggregates,[8,38] our result indicates that the ionic side groups in the hard domains do not orient significantly in the plane of the film during the deformation.

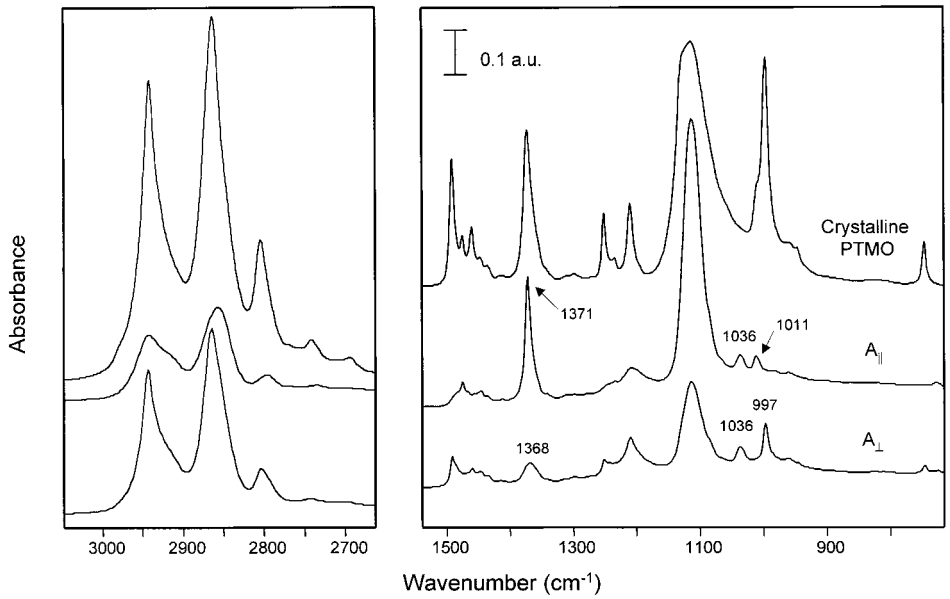

Figure 2. FTIR spectrum of crystalline PTMO and polarized FTIR spectra of the PTMO zwitterionomer at a draw ratio of 5.6, measured with radiation polarized parallel ($A_{\|}$) and perpendicular ($A_{\perp}$) to the stretch direction at ambient temperature.

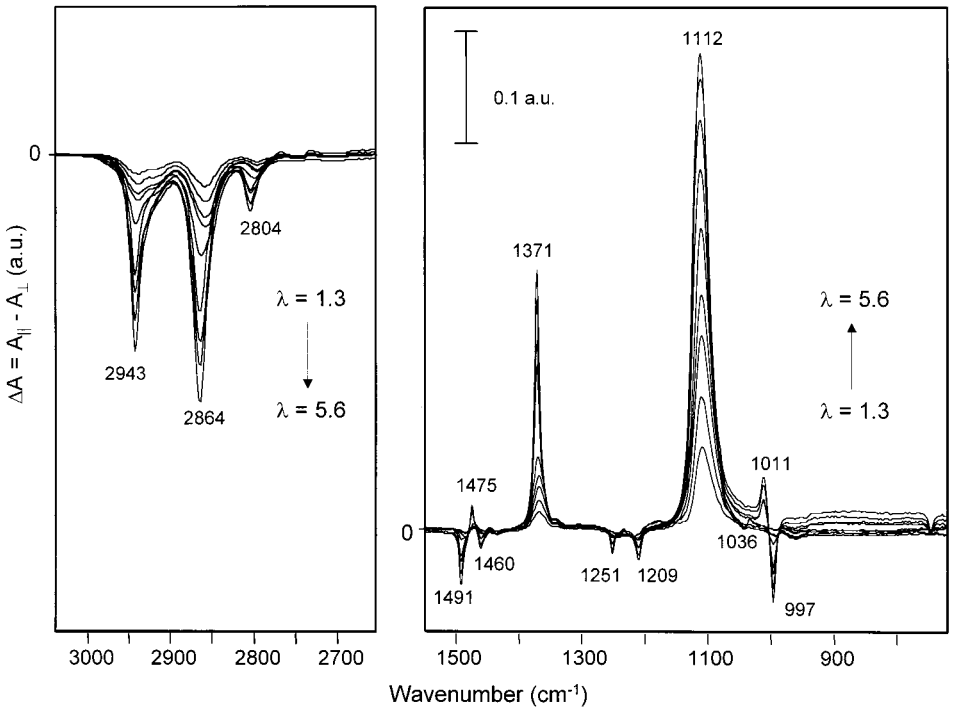

Figure 3. Dichroic difference spectra ($\Delta A = A_{\|} - A_{\perp}$) of the PTMO zwitterionomer measured at draw ratios of 1.3, 1.7, 2.3, 2.8, 3.4, 4.0, 4.5, 4.9, and 5.6 at ambient temperature.

Because the 1036 cm^{-1} band is not sensitive to crystallization and well separated from other bands, its isotropic absorbance is also useful for calibrating the film thickness variation during stretching of the sample. For this, the following expression was used:

$$A_0(\lambda) = (A_{\|}(\lambda) + 2A_{\perp}(\lambda))/3 \qquad (2)$$

where $A_{\|}(\lambda)$ and $A_{\perp}(\lambda)$ are the absorbances of the band at a draw ratio of λ, measured with the polarized infrared radiation parallel and perpendicular to the stretch direction, respectively. Figure 4 shows the effects of the draw ratio on the isotropic absorbance of the 1036 cm^{-1} band for the three elongation−retraction cycles. It can be seen that the film thickness is reversible in the elongation−retraction cycles. It is also noted that the film does not completely recover the original length, indicative of some flow in this process.

Even though the bands due to the CH_2 stretching and bending vibrations in the 3000−2750 and 1470−1400 cm^{-1} ranges, respectively, show considerable dichroism, they were not used for further analysis in the current study because of strong overlap. Instead, the focus in the following is on the PTMO bands due to the C−O−C antisymmetric stretching mode at about 1112 cm^{-1} and especially the CH_2 wagging mode at about 1368 cm^{-1}, both of which are more isolated from other bands.

Figure 5 shows the change in peak position of the parallel polarized absorption at about 1112 cm^{-1} for the three elongation−retraction cycles. It is observed that

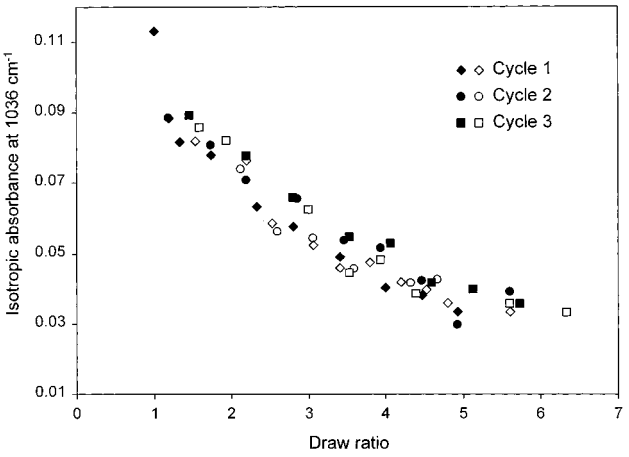

Figure 4. Variation of the isotropic absorbance of the band at about 1036 cm^{-1} during stretch (filled symbols) and recovery (open symbols) in three elongation−retraction cycles.

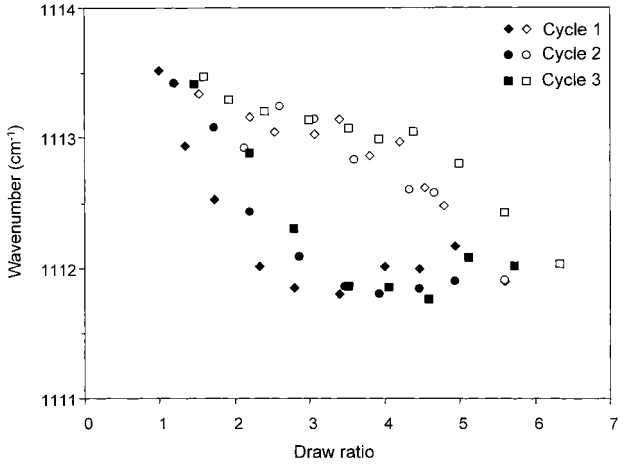

Figure 5. Variation of the position of the band at about 1112 cm^{-1} during stretch (filled symbols) and recovery (open symbols) in three elongation−retraction cycles.

the band position decreases until a draw ratio of about 3 is reached, after which, coinciding with the onset of crystallization, it remains relatively constant. The peak position reverts back after the release of the strain, but with a significant hysteresis. On the other hand, the peak position of the perpendicularly polarized absorption shows no significant shift with deformation of the polymer. The cyclic variation of the parallel-polarized peak position is most likely due to a change in bond strength during the elongation−retraction processes. This can be related to stress on the bond coordinates that provides the force for the recovery of the film length after releasing the external stress. Changes in the bond stress affecting the position of the parallel-polarized 1112 cm^{-1} band appear to take place during stretching only before any crystallization occurs.

To address the segmental behavior in the amorphous phase, the amorphous band at 1368 cm^{-1}, for which no change in band position is detected, was used. This relatively broad band can be resolved from the sharp crystalline peak at 1371 cm^{-1} by curve fitting. Since the latter appears only in the parallel polarized spectra, the difference between the parallel and perpendicularly polarized spectra can be used to determine the shape and peak position of the crystalline band at 1371 cm^{-1}. The difference spectrum was calculated by adjusting the subtraction factor until there was complete disappearance of the broad band at 1368 cm^{-1}. The shape and position of the 1368 cm^{-1} band used for the curve fitting was determined from the perpendicular spectrum. The curve fitting of the 1300−1400 cm^{-1} region also revealed the presence of two small bands at 1355 and 1340 cm^{-1}. These weak bands cannot be assigned confidently but may arise from different conformations or from the CH_2 groups in or near the zwitterionic moieties. A typical example of curve fitting for the parallel polarized spectrum at a draw ratio of 5.6 in the first elongation−retraction cycle is shown in Figure 6. It should be noted that the band at 1371 cm^{-1} is very close to a Lorenzian line shape, while the other three components are close to a Gaussian line shape. By curve fitting the parallel polarized spectra, it was possible to determine the intensities of the 1371 and 1368 cm^{-1} bands as a function of draw ratio.

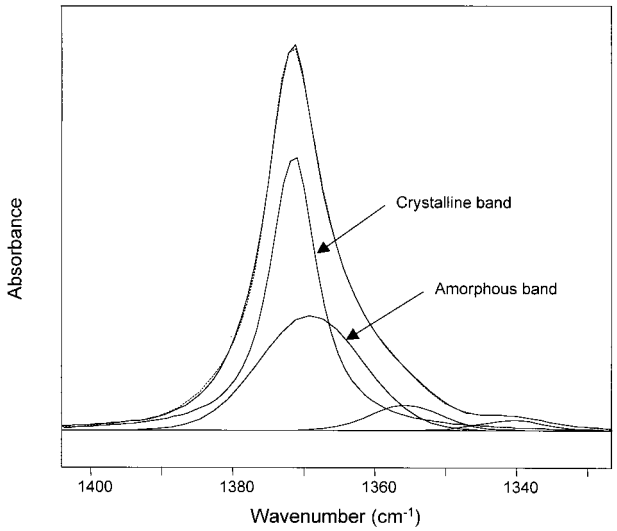

Figure 6. Example of the curve fitting of the parallel polarized absorption band at about 1368 cm^{-1} for a film drawn at $\lambda = 5.6$. The solid and dashed lines represent the experimental and fitted spectra, respectively.

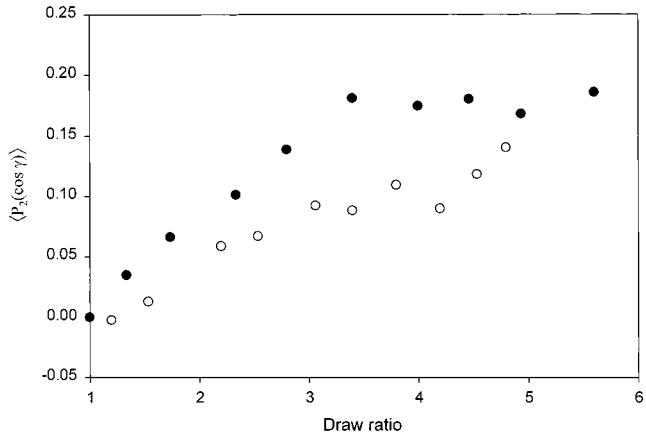

Figure 7. Variation of the orientation function $\langle P_2(\cos \gamma)\rangle$ calculated from the band at about 1368 cm^{-1} during stretch (filled symbols) and recovery (open symbols) in the first elongation−retraction cycle.

Figure 7 shows the variation of the orientation function $\langle P_2(\cos \gamma)\rangle$ calculated from the band at 1368 cm^{-1} in the first elongation−retraction cycle. It is observed that the orientation function initially increases linearly with draw ratio and then reaches a plateau near the draw ratio of about 3, where crystallization begins. Thus, there is no further orientation of the amorphous

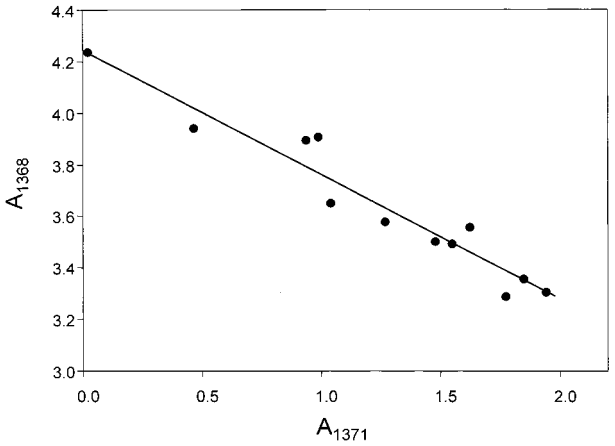

Figure 8. Relationship between the normalized isotropic absorbance of the bands at 1371 and 1368 cm^{-1} in the crystallization process of the first elongation−retraction cycle.

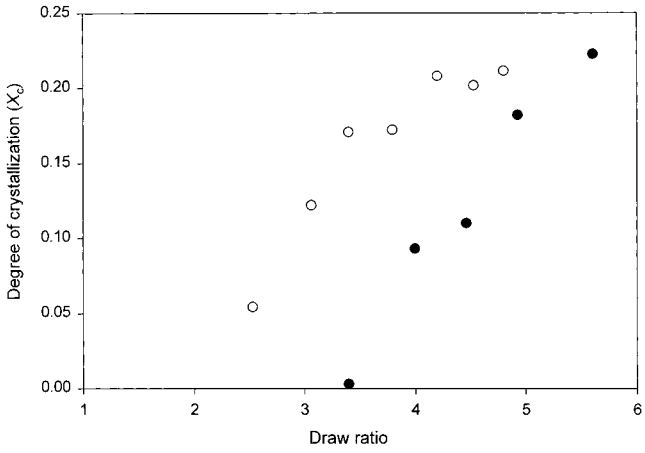

Figure 9. Variation of the degree of crystallization during stretch (filled symbols) and recovery (open symbols) in the first elongation−retraction cycle.

segments once crystallization occurs. Instead, the sufficiently oriented amorphous PTMO segments transfer to the crystalline region, and the sharp absorption at 1371 cm^{-1} increases at the expense of the broader one at 1368 cm^{-1}. It is noted that the orientation required for crystallization appears to be quite low, as was also found, for example, in the orientation studies of linear low-density polyethylene.[43] When the strain is released after attaining a draw ratio of 5.6, the orientation decreases continuously, and the orientation function is always lower than that for the same draw ratio during the stretch process. These results are in accordance with the wavenumber variation and hysteresis behavior shown in Figure 5. Thus, the increase in orientation of the amorphous phase until the onset of crystallization leads to an increase in tension of the valence coordinates, causing the band position to move to lower wavenumbers, and the band recovers its original position with disappearance of the orientation.

The degree of crystallization of the deformed PTMO zwitterionomer can be obtained from the relative intensities of the bands at 1368 and 1371 cm^{-1} if the molar absorptivities of the two bands are known. The relationship between the intensities of the two bands can be expressed by the following equation:

$$\frac{A^0_{1368}}{\epsilon_{1368}} = \frac{A_{1368}}{\epsilon_{1368}} + \frac{A_{1371}}{\epsilon_{1371}} \tag{3}$$

where A_{1371} and A_{1368} represent the isotropic absorbances of the bands at 1371 and 1368 cm^{-1}, respectively, after normalization for the film thickness using the 1036 cm^{-1} band as an internal intensity standard, A^0_{1368} is the normalized isotropic absorbance of the band at 1368 cm^{-1} when the sample is purely amorphous ($A_{1371} = 0$), and ϵ are the molar absorptivities. Equation 3 can be rearranged to give

$$A_{1368} = A^0_{1368} - bA_{1371} \tag{4}$$

where b is the ratio of the molar absorptivities of the 1368 and 1371 cm^{-1} bands ($\epsilon_{1368}/\epsilon_{1371}$).

Figure 8 shows the relationship between the normalized isotropic absorbances of the 1371 and 1368 cm^{-1} bands in the crystallization process of the first elongation−retraction cycle. A slope of 0.49 was found by a least-squares fit to the data in Figure 8, showing that

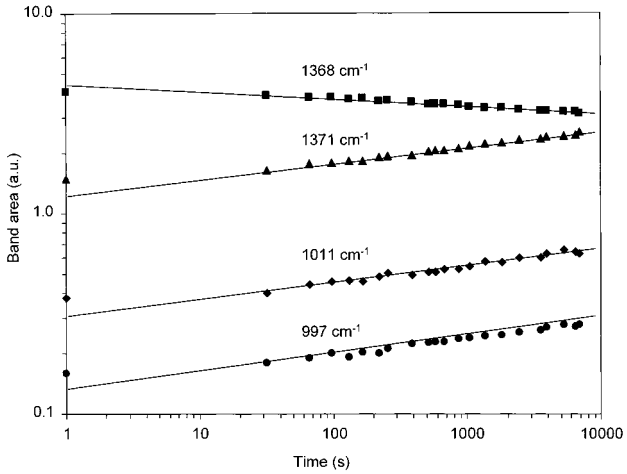

Figure 10. Effect of time on the intensity of the bands at 997, 1011, 1371, and 1368 cm^{-1} after fast stretching the PTMO zwitterionomer to a draw ratio of 2.8 at ambient temperature.

the molar absorptivity of the 1371 cm^{-1} band is about twice that of the 1368 cm^{-1} band. The degree of crystallization, X_c, can therefore be calculated using the following equation:

$$X_c = \frac{bA_{1371}}{bA_{1371} + A_{1368}} \tag{5}$$

Figure 9 shows the variation in degree of crystallization as a function of draw ratio in the first elongation−retraction cycle. The highest degree of crystallization in the elongation−retraction process is about 22%. In comparison, the degree of crystallization in this zwitterionomer in its unoriented state, as determined by DSC, is about 17%.[9]

As pointed out previously, strain-induced crystallization is not a thermodynamic equilibrium process.[15] At constant strain, the degree of crystallization increases and the orientation of the amorphous regions changes as a function of time. This dynamic process was monitored by stretching the film rapidly to a draw ratio of 2.8 at ambient temperature and then measuring the change of orientation and crystallization. Figure 10 shows the intensity variations of the bands at 997, 1011, 1368, and 1371 cm^{-1} as a function of time on a logarithmic scale. It is observed that the intensity of the

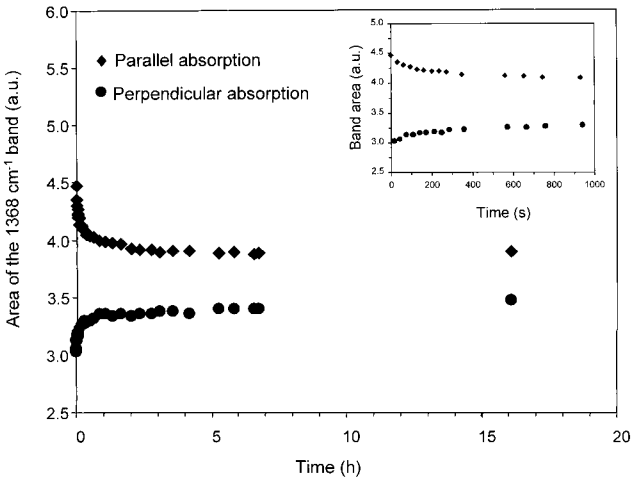

Figure 11. Effect of time on the parallel and perpendicular polarized absorbance of the band at about 1368 cm^{-1} after fast stretching the PTMO zwitterionomer to a draw ratio of 2.8 at 40 °C.

three crystalline bands at 1371, 1011, and 997 cm^{-1} shows a parallel behavior with time. The intensity of the amorphous band at 1368 cm^{-1} decreases as a function of time. These trends confirm the soundness of the curve-fitting procedure used. Figure 10 also shows that the crystallization kinetics during the experimental time scale follow the Avrami equation:

$$\ln X_c = \ln K_c + n \ln t \qquad (6)$$

where K_c is the crystallization rate constant and n is the Avrami exponent, which is a characteristic quantity for a certain type of nucleation and crystal growth. The fitting of the data in Figure 10 gives a value of 0.8 for n. This value corresponds to one-dimensional crystal growth with heterogeneous athermal nucleation.[15]

Orientation Relaxation. The orientation relaxation behavior of the zwitterionomer, stretched at draw ratios and temperatures where strain-induced crystallization is avoided, was also investigated. A typical example of results obtained is shown in Figure 11: the zwitterionomer film was stretched rapidly to a draw ratio of 2.8 at 40 °C, and the variation of the parallel and perpendicular infrared absorbances at 1368 cm^{-1} was followed as a function of time. Because of orientation relaxation, the intensity of the parallel and perpendicular absorbances decreases and increases as a function of time, respectively. Since the two orthogonally polarized spectra are shifted by about 12 s, the intensities of the perpendicular infrared absorbances at times corresponding to the parallel polarized spectra were obtained by interpolation in order to calculate the dichroic ratios.

Figure 12 shows the orientation relaxation behavior of the 1368 cm^{-1} band at 35, 47, and 60 °C and that of the 1036 cm^{-1} band at 47 °C. Because of the experimental setup used, the relaxation behavior at times shorter than 30 s could not be determined confidently. In any case, the relaxation in the short time range involves fast relaxation such as Rouse movements and is not the object of the current study. In this figure, the band at about 1036 cm^{-1}, associated with the ionic aggregates, shows very low orientation and no detectable relaxation. Despite the low orientation, it was observable that the values of the orientation function tended to decrease with increasing temperature. Furthermore, relaxation became increasingly visible for the curves at 55 and 60 °C.

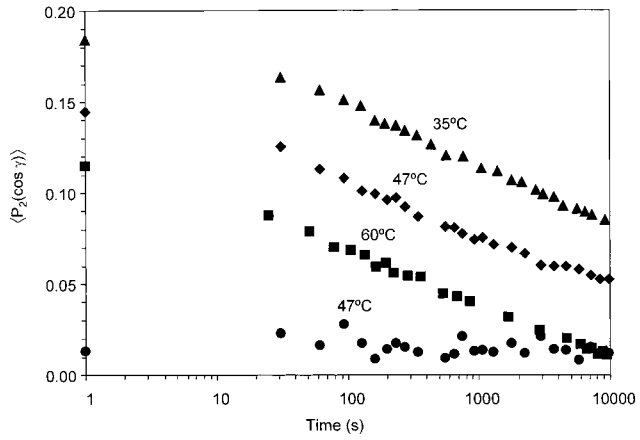

Figure 12. Orientation relaxation after fast stretching the PTMO zwitterionomer to a draw ratio of 2.8, determined from the 1368 cm^{-1} band at 35 °C (▲), 47 °C (◆), and 60 °C (■) and from the 1036 cm^{-1} band at 47 °C (●).

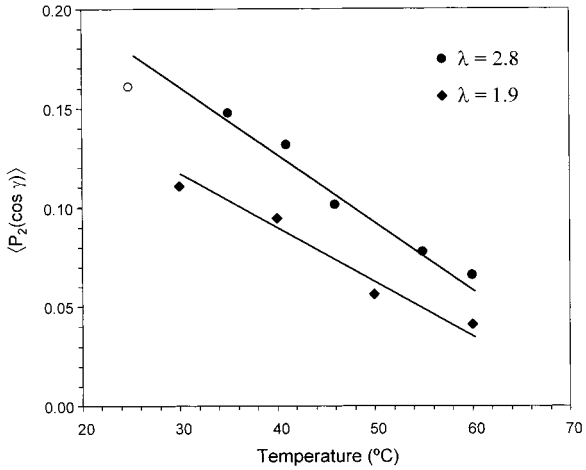

Figure 13. Temperature dependence of the orientation function $\langle P_2(\cos\gamma)\rangle$ calculated from the 1368 cm^{-1} band at 140 s after fast stretching the zwitterionomer to draw ratios of 1.9 and 2.8. The open circle is for the partly crystallized sample stretched to a draw ratio of 2.8 at ambient temperature (obtained from the data in Figure 10).

The band at about 1368 cm^{-1}, due to the PTMO soft domains, shows much higher orientation and clearly relaxes as a function of time. It was found that the relaxation curves obtained from this band cannot be fitted by a single-exponential decay; this indicates the existence of multiple relaxations with different rate constants in this process.[44−46] Figure 12 also shows that the level of orientation indicated by the 1368 cm^{-1} band decreases with temperature. At 60 °C, it decreases to nearly zero in about 3 h. The decrease in orientation with temperature is shown for a greater number of temperatures in Figure 13, where the samples were rapidly stretched to draw ratios of 1.9 and 2.8. The point for the ambient temperature experiment of Figure 10 is also included, although the sample is partly crystallized in this case. The orientation function used in this figure is the value after orientation relaxation of about 140 s. It is observed that the orientation function appears to decrease with temperature in an approximately linear manner in the range studied.

Finally, the various relaxation curves for the 1368 cm^{-1} band obtained after fast stretching to a draw ratio

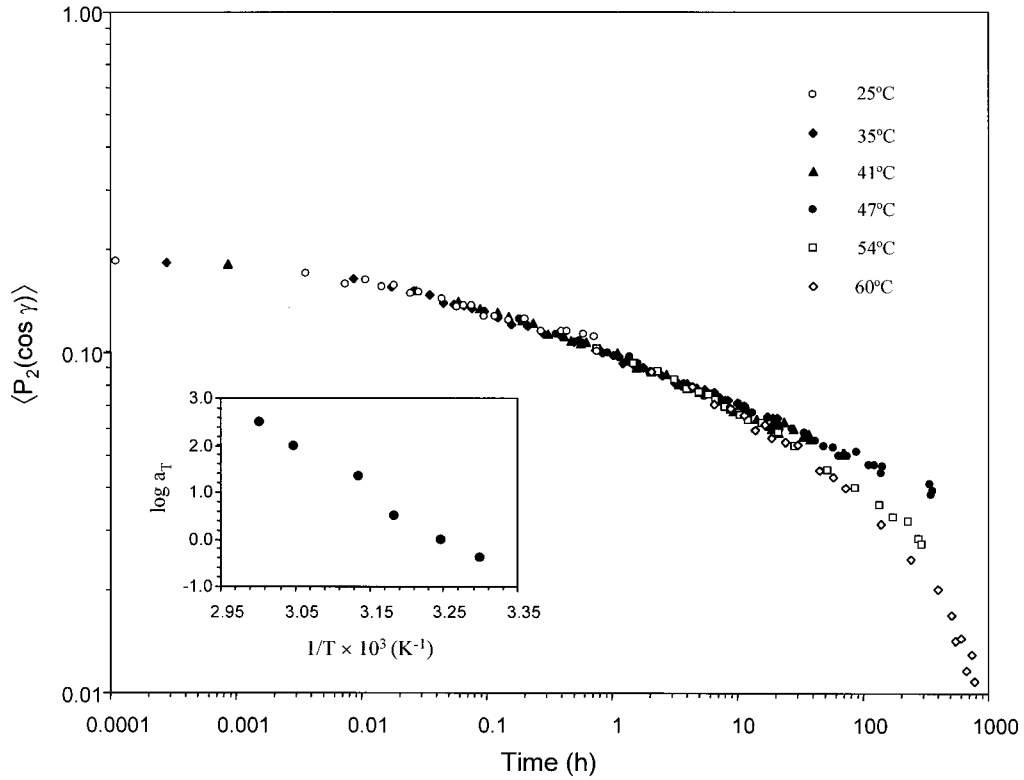

Figure 14. Time−temperature superposition, giving a pseudo-master curve, of the orientation relaxation curves using 35 °C as the reference temperature. The inset shows the variation of the shift factors with inverse temperature.

of 2.8 were superposed according to the time−temperature superposition principle, using 35 °C as the reference temperature. No vertical shift factors were included. The master curve obtained is shown in Figure 14. The relaxation curves for 35, 41, and 47 °C could be completely overlapped. The ambient temperature curve shows a very short long-time tail that does not quite superpose on the master curve and may be related to the crystallization in this sample. The two highest temperature curves at 54 and 60 °C were fitted to the master curve by overlapping as much as possible of the shorter-time region, leaving fairly lengthy tails where superposition is not possible (although vertical shift factors of 2.0 and 2.3, respectively, do allow very good superposition of those two curves).

Failure of time−temperature superposition is frequently observed in biphasic ionomers,[1] notably in stress relaxation experiments.[47,48] In the present case, it is noteworthy that good to excellent superposition is obtained for all the curves below or well within the hard-phase (cluster) T_g (located at about 44 °C; see Experimental Section) and fails for the temperatures significantly above the midpoint of this T_g. It is for these same temperatures that some relaxation is detected in the ionic sulfonate groups, as mentioned above. It may be added that the shift factors for the superposition in Figure 14, shown in the form of an Arrhenius plot in the inset of this figure, yield an apparent Arrhenius activation energy of 190 kJ/mol.

The relaxation of the PTMO segments in the stretched samples contrasts with the form of the rubbery plateau obtained in DMA measurements (reminiscent of covalently cross-linked rubbers up to about 100 °C; see Introduction and Experimental Section). Possibly, this is related to the much greater deformation in the present experiments compared to the dynamic mechanical experiments. Since the zwitterionomers are hygroscopic materials, it is also not ruled out that there is (more) residual water in the sample of the present study compared to that used in the DMA study. It is well-known that polar molecules plasticize ionic aggregates and increase the rate of ion-hopping in ionomers.[49]

SAXS investigations of a zwitterionomer analogous to the one of this study indicate that the ionic aggregates are hexagonally arranged in cylindrical structures, which orient perpendicularly to the plane of the film when uniaxially stretched.[38] If the polymer of the present study behaves in the same way, the cylinders become oriented with their axis in the direction of the infrared beam, presumably with the sulfonate groups distributed isotropically around the cylinder axis. This could account for the very low orientation observed from the sulfonate bands.

Conclusions

Orientation and strain-induced crystallization in a segmented PTMO zwitterionomer with elastomeric characteristics were studied by infrared linear dichroism. It was found that the crystallized segments are almost perfectly oriented with their chain axis in the direction of strain. By using curve fitting, it was possible to follow the orientation behavior of the amorphous phase in the cyclic elongation−retraction experiments. It was found to increase in a roughly linear manner until sufficient for crystallization to begin (at a relatively low level of orientation), after which it remains constant. With stepwise release of stress, the amorphous phase orientation decreases steadily to zero in the whole range of stress. The degree of crystallization as a function of draw ratio was also determined, reaching 22% for a draw ratio of 5.6, and is completely reversible although with hysteresis. The crystallization kinetics was shown to be consistent with one-dimensional growth.

At temperatures and draw ratios where no crystallization is induced, orientation relaxation occurs. The PTMO orientation decreases and the relaxation rate increases with increasing temperature. Very good time−temperature superposition of the curves is possible at all but the highest temperatures, which can be correlated with the hard phase glass transition temperature. Only very low orientation and relaxation can be detected in the ionic regions.

Acknowledgment. The financial support of the Natural Sciences and Engineering Research Council of Canada (NSERC) and the Fonds pour la Formation de Chercheurs et Aide à la Recherche (FCAR) is acknowledged. We are grateful to Drs. J.-C. Galin and B. Grassl for their generous gift of the zwitterionomer.

References and Notes

(1) Eisenberg, A., Kim, J.-S., Eds.; *Introduction to Ionomers;* John Wiley & Sons: New York, 1998.
(2) Tant, M. R., Mauritz, K. A., Wilkes, G. L., Eds.; *Ionomers: Synthesis, Structure, Properties, and Application;* Blackie Academic and Professional (Chapman & Hall): New York, 1997.
(3) Schlick, S., Ed.; *Ionomers: Characterization, Theory and Applications;* CRC Press: Boca Raton, FL, 1996.
(4) Eisenberg, A.; Hird, B.; Moore, R. B. *Macromolecules* **1990**, *23*, 4098.
(5) Galin, J. C. Polyzwitterions (Overview). In *Polymer Materials Encyclopedia*; Salamone, J. C., Ed.; CRC Press: Boca Raton, FL, 1996; Vol. 9, p 7189.
(6) Grassl, B.; Galin, J. C. *Macromolecules* **1995**, *28*, 7035.
(7) Grassl, B.; Meurer, B.; Scheer, M.; Galin, J. C. *Macromolecules* **1997**, *30*, 236.
(8) Grassl, B.; Mathis, A.; Rawiso, M.; Galin, J.-C. *Macromolecules* **1997**, *30*, 2075.
(9) Vuillaume, P. Y. M.Sc. Thesis, Chemistry Department, Laval University, Québec, 1996; to be published.
(10) Siesler, H. W. *Adv. Polym. Sci.* **1984**, *65*, 1.
(11) Treloar, L. R. G. *The Physics of Rubber Elasticity;* Oxford University Press: New York, 1958.
(12) Kajiyama, T.; Stein, R. S.; MacKnight, W. J. *J. Appl. Phys.* **1970**, *41*, 4361.
(13) Kajiyama, T.; Oda, T.; Stein, R. S.; MacKnight, W. J. *Macromolecules* **1971**, *4*, 198.
(14) Enderle, H. F.; Kilian, H. G.; Heise, B.; Mayer, J.; Hespe, H. *Colloid Polym. Sci.* **1986**, *264*, 305.
(15) Stadler, R.; Gronski, W. *Colloid Polym. Sci.* **1986**, *264*, 323.
(16) Ding, Y. S.; Register, R. A.; Yang, C.; Cooper, S. L. *Polymer* **1989**, *30*, 1204.
(17) Holl, B.; Kilian, H. G.; Schenk, H. *Colloid Polym. Sci.* **1990**, *268*, 205.
(18) Battjes, K. P.; Kuo, C.-M.; Miller, R. L.; Saam, J. C. *Macromolecules* **1995**, *28*, 790.
(19) McLean, R. S.; Sauer, B. B. *J. Polym. Sci., Part B: Polym. Phys.* **1999**, *37*, 859.
(20) Tassin, J. F.; Monnerie, L. *J. Polym. Sci., Part B: Polym. Phys. Ed.* **1983**, *21*, 1981.
(21) LeBourvellec, G.; Monnerie, L.; Jarry, J. P. *Polymer* **1986**, *27*, 856.
(22) Deloche, B.; Beltzung, M.; Herz, J. *J. Phys., Lett.* **1982**, *43*, 763.
(23) Uemura, Y.; Stein, R. S.; MacKnight, W. J. *Macromolecules* **1971**, *4*, 490.
(24) Seymour, R. W.; Allegrezza, A. E., Jr.; Cooper, S. L. *Macromolecules* **1973**, *6*, 896.
(25) Allegrezza, A. E., Jr.; Seymour, R. W.; Ng, H. N.; Cooper, S. L. *Polymer* **1974**, *15*, 433.
(26) Jasse, B.; Koenig, J. L. *J. Macromol. Sci., Rev. Macromol. Chem.* **1979**, *C17*, 61.
(27) Siesler, H. W. *Colloid Polym. Sci.* **1984**, *262*, 223.
(28) Ylitalo, C. M.; Kornfield, J. A.; Fuller, G. G.; Pearson, D. S. *Macromolecules* **1991**, *24*, 749.
(29) Walczak, W. J.; Wool, R. P. *Macromolecules* **1991**, *24*, 4657.
(30) Besbes, S.; Cermelli, I.; Bokobza, L.; Monnerie, L.; Bahar, I.; Erman, B.; Herz, J. *Macromolecules* **1992**, *25*, 1949.
(31) Fan, X.-D.; Bazuin, C. G. *Macromolecules* **1993**, *26*, 2508.
(32) Fan, X.-D.; Bazuin, C. G. *Macromolecules.* **1995**, *28*, 8216.
(33) Bazuin, C. G.; Fan, X.-D. *Macromolecules* **1998**, *31*, 1321.
(34) Sherman, B. J.; Neaffer, R. O.; Galiatsatos, V. *Trends Polym. Sci.* **1996**, *4*, 72.
(35) Bokobza, L.; Lapra, A. *J. Polym. Sci., Part B: Polym. Phys.* **2000**, *38*, 2449.
(36) Pellerin, C.; Prud'homme, R. E.; Pézolet, M. *Macromolecules* **2000**, *33*, 7009.
(37) Messé, L.; Pézolet, M.; Prud'homme, R. E. *Polymer* **2001**, *42*, 563.
(38) Grassl, B. Ph.D. Thesis, Institut Charles Sadron, Université Louis Pasteur, Strasbourg, 1995.
(39) Cameron, D. G.; Kauppinen, J. K.; Moffatt, D. J.; Mantsch, H. H. *Appl. Spectrosc.* **1982**, *36*, 245.
(40) Buffeteau, T.; Pézolet, M. Linear Dichroism in Infrared Spectroscopy. In *Handbook of Vibrational Spectroscopy*; Chalmers, J., Griffiths, P. R., Eds.; Wiley-VCH: London, 2001.
(41) Matsui, Y.; Kubota, T.; Tadokoro, H.; Yoshihara, T. *J. Polym. Sci., Part A* **1965**, *3*, 2275.
(42) Yokoyama, M.; Ochi, H.; Tadokoro, H.; Price, C. C. *Macromolecules* **1972**, *5*, 690.
(43) Seguela, R.; Rietsch, F. *Polymer* **1986**, *27*, 532.
(44) Palmer, R. G.; Stein, D. L.; Abrahams, E.; Anderson, R. W. *Phys. Rev. Lett.* **1984**, *53*, 958.
(45) Serero, Y.; Jacobsen, V.; Berret, J. F.; May, R. *Macromolecules* **2000**, *33*, 1841.
(46) Clément, F.; Johner, A.; Joanny, J.-F.; Semenov, A. N. *Macromolecules* **2000**, *33*, 6148.
(47) Eisenberg, A.; Navratil, M. *J. Polym. Sci., Polym. Lett.* **1972**, *10*, 537.
(48) Eisenberg, A.; Navratil, M. *Macromolecules* **1973**, *6*, 604.
(49) See, for example, the review: Bazuin, C. G. *ACS Symp. Ser.* **1989**, *395*, 476.

MA0107197